Processing of recombinant AAV genomes occurs in specific nuclear structures that overlap with foci of DNA-damage-response proteins

Tiziana Cervelli[1,*], Jose Alejandro Palacios[2,*], Lorena Zentilin[2], Miguel Mano[2], Rachel A. Schwartz[3], Matthew D. Weitzman[3] and Mauro Giacca[1,2,‡]

[1]Molecular Biology Laboratory, Scuola Normale Superiore, AREA della Ricerca del CNR, Via Moruzzi 1, Pisa, Italy
[2]Molecular Medicine Laboratory, International Centre for Genetic Engineering and Biotechnology (ICGEB), Padriciano 99, Trieste, Italy
[3]Laboratory of Genetics, The Salk Institute for Biological Studies, La Jolla, CA 92037, USA

*These authors contributed equally to this work
‡Author for correspondence (e-mail: giacca@icgeb.org)

Accepted 30 October 2007
J. Cell Sci. 121, 349-357 Published by The Company of Biologists 2008
doi:10.1242/jcs.003632

Summary

Despite increasing utilization of rAAV vectors in gene transfer applications, several aspects of the biology of these vectors remain poorly understood. We have visualized the conversion of rAAV vector genomes from single-stranded to double-stranded DNA in real time. We report that rAAV DNA accumulates into discrete foci inside the nucleus. These rAAV foci are defined in number, increase in size over time after transduction, are relatively immobile, and their presence correlates with the efficiency of cell transduction. These structures overlap with, or lie in close proximity to, the foci in which proteins of the MRN (MRE11-RAD50-NBS1) complex as well as the MDC1 protein accumulate after DNA damage. The downregulation of MRN or MDC1 by RNA interference markedly increases both the formation of rAAV foci and the extent of rAAV transduction. Chromatin immunoprecipitation experiments indicate that the MRE11 protein associates with the incoming rAAV genomes and that this association decreases upon cell treatment with DNA damaging agents. These findings are consistent with a model whereby cellular DNA-damage-response proteins restrict rAAV transduction by negatively regulating rAAV genome processing.

Supplementary material available online at
http://jcs.biologists.org/cgi/content/full/121/3/349/DC1

Key words: AAV, DNA repair, MRN complex, Viral vectors

Introduction

The adeno-associated virus (AAV) is a replication defective parvovirus with a single-stranded (ss) DNA genome flanked by two short self-complementary palindromic sequences (inverted terminal repeats, ITRs). Recombinant AAV (rAAV) vectors are easily produced by replacing the whole viral genome with the gene of interest, with the exception of the ITRs, which contain all the cis-acting elements necessary for replication and packaging (Hermonat and Muzyczka, 1984; Tratschin et al., 1984).

Although the utilization of rAAV vectors in pre-clinical and clinical gene transfer applications is rising, several aspects of the life cycle of both the wild-type virus and, most notably, of the recombinant vectors remain largely obscure. In particular, limited information is available on the intracellular fate of rAAV DNA after internalization. This appears to be a topic of particular relevance considering that a relatively small number of tissues are permissive to rAAV transduction, despite the receptors for AAV internalization being widespread in most cell types in vivo.

In cultured cells, a marked increased in rAAV transduction efficiency is obtained by treating cells with agents that affect genomic DNA integrity or metabolism, such as UV irradiation, hydroxyurea (HU), topoisomerase inhibitors and several chemical carcinogens (Alexander et al., 1994; Russell et al., 1995; Zentilin et al., 2001; Zhou et al., 1999). A major effect of these treatments is the improved conversion of the input vector ssDNA genome into double-stranded (ds) DNA (Ferrari et al., 1996; Fisher et al., 1996), which represents an essential requisite for gene expression. These observations have raised the possibility that permissivity to rAAV transduction might be related to the induction of the cellular DNA-damage response (DDR) and, in particular, of the proteins involved in DNA-double-strand break (DSB) repair (Zentilin et al., 2001).

In eukaryotic cells, surveillance mechanisms have evolved to rapidly recognize DNA damage and signal its presence. In particular, the occurrence of DSBs in chromosomal DNA elicits a signaling response through the ataxia-telangiectasia mutated (ATM) protein kinase, which coordinates cell-cycle arrest, DNA repair and apoptosis (Shiloh, 2003). Recent evidence indicates that the MRE11-RAD50-NBS1 (MRN) complex is an essential mediator of ATM recruitment to, and activation by, DSBs, both by forming multiple protein-protein contacts with ATM (Lee and Paull, 2005) and by tethering damaged DNA, thereby increasing its local concentration (Dupre et al., 2006). The retention of MRN at the DSB sites requires direct binding of its NBS1 component to the mediator of DNA damage checkpoint protein 1 (MDC1) (Goldberg et al., 2003; Lukas et al., 2004; Stewart et al., 2003).

In response to DNA damage, several components of the DDR, normally diffuse in the nucleoplasm, are rapidly relocalized and concentrated into subnuclear compartments that are microscopically detected as foci. Although the exact nature of the molecular processes occurring at these foci is still not completely understood, experimental evidence indicates that at least some of these foci form in correspondence or in close proximity to the sites

of actual DNA damage and that the increase local concentration of factors they determine is beneficial for genome surveillance and repair (Seno and Dynlacht, 2004; van den Bosch et al., 2003).

Essential to comprehend the mechanisms of rAAV genome processing is the understanding of the intracellular fate of vector genomes after cell transduction. In this respect, recent studies have demonstrated the feasibility of visualizing specific genomic regions within the nucleus by exploiting the interaction of sequence-specific DNA-binding proteins linked to the green fluorescent protein (GFP) with tandem repeats of cognate binding sites. In particular, different studies have employed a system based on the bacterial Lac operator-repressor (LacO/R) interaction to examine chromatin organization, separation of sister chromatids, chromosome dynamics and gene expression in living cells (Belmont and Straight, 1998; Straight et al., 1997; Tsukamoto et al., 2000; Tumbar et al., 1999). This procedure has also proved useful in the study of wild-type AAV replication in the presence of helper virus (Fraefel et al., 2004; Glauser et al., 2005).

In this work, we adapted the LacO/R system for the visualization in real time of the sites of ssDNA to dsDNA conversion of rAAV vector genomes inside the nucleus of the transduced cell, in the absence of helper virus or of any other helper gene products. We observed that rAAV DNA accumulates in discrete foci inside the nucleus, which increase in size and are relatively immobile over time. These rAAV foci lie in close proximity to the foci in which proteins of the MRN complex and MDC1 accumulate after DNA damage. We also report that silencing of NBS1 and MDC1 by RNA interference markedly enhances rAAV transduction, indicating that MRN and MDC1 play an inhibitory role on rAAV genome processing. These findings support the conclusion that these cellular DDR proteins significantly restrict rAAV transduction.

Results

Visualization of the nuclear sites of dsAAV DNA formation in live cells

To address the study of the kinetics of cell transduction with rAAV and, most notably, to visualize the fate of rAAV genomes in living cells, we constructed a rAAV vector (AAVLacO.14), carrying 112 LacR binding sites (LacO repeats) cloned between the viral ITRs; this vector was used to infect HeLa and MRC5 cell lines that stably express a GFP-LacR fusion protein with a C-terminal nuclear localization signal (HeLa/GFP-LacR and MRC5/GFP-LacR cells). The rationale of this approach is that the fluorescent sequence-specific DNA binding protein only binds its target sites when these are present in a dsDNA form, thus allowing the dynamic visualization of dsDNA formation over time (Fig. 1A).

Movie 1 in the supplementary material shows infection of MRC/GFP-LacR cells over a 24-hour period; frames from this movie are shown in Fig. 1B. We found that the generation of ds rAAV DNA was not diffused throughout the nucleus but appeared restricted to specific nuclear sites. These rAAV foci were detected as early as 3 hours post infection (p.i.) as tiny bright spots within the diffuse GFP-LacR background signal inside the nucleus and then expanded into larger structures over time. The formation of rAAV foci was more evident after cell treatment with hydroxyurea (HU), a drug inducing dsDNA breaks when used in the mM range, or other genotoxic agents known to increase rAAV transduction (Fig. 1C). No foci were ever detected in the absence of rAAV infection or upon transduction with other rAAVs that do not contain the LacO target sequences (e.g. AAV-LacZ; Fig. 1C), irrespective of any genotoxic treatment.

Time-lapse imaging studies performed in living infected cells in order to track the movement of individual foci indicated that these structures were relatively immobile and only displayed an apparently random movement in a relatively restricted area of the nucleus (supplementary material Fig. S1A-D). These experiments also revealed that the intensity of fluorescence of individual foci progressively increased over the first 8-10 hours p.i. (supplementary material Fig. S1E), suggestive of a progressive accumulation of dsDNA rAAV genomes into these structures.

Quantitative analysis of rAAV formation indicated that the percentage of cells showing rAAV foci increased during the first 24 hours p.i.; at all times, this number was higher after treatment with HU; 25.1±9.2% and 11.9±0.6% cells with foci in HU-treated and untreated cells, respectively, at 24 hours; Fig. 2A). The number of AAVLacO.14 foci per cell nucleus was also determined in 3D-images of 30-60 nuclei observed over time (Fig. 2B). The maximum number of foci was detected at 24 hours p.i. in HU-treated cells (23.9±19.1 foci per nucleus) and at 8 hours in untreated cells (12.1±9.6). Interestingly, the number of rAAV foci only modestly increased at these times compared with the earlier time points, suggesting that their number per cell was determined very soon after infection. Finally, rAAV foci progressively disappeared at later time points, even if some foci were found to persist as long as 6 days in both HU-treated and untreated cells (data not shown).

To obtain an estimate of the number of rAAV genomes per focus, we infected cells with a rAAV vector expressing the *lacZ* gene and assessed the amount of viral genomes present inside the nucleus at different times after infection by real-time PCR. The purity of the nuclear fractions was confirmed by western blotting against cytoplasmic α-tubulin and nuclear poly (ADP-ribose) polymerase (PARP) proteins (supplementary material Fig. S2). We found that the number of rAAV genomes inside the nucleus progressively increased up to 12 hours in HU-treated cells, reaching a maximum of over 400 genomes/nucleus; in non-treated cells, the number of genomes at 12 hours p.i. was less than half this amount (Fig. 2C). Considering the number of foci per cell observed under similar conditions, and assuming that all rAAV DNA clusters form rAAV foci, these data indicate that, on average, each rAAV focus is composed of no more than ~20 viral genomes. In agreement with these results, through the comparison of the GFP fluorescence intensity of rAAV foci with that of GFP-tagged rotavirus [virus-like particles containing a known number of GFP molecules (Dundr et al., 2002)], we estimated that the great majority of the observed rAAV foci (>80%) contained one to ten vector genomes, with a range of estimated genomes per foci that varied from one to 250 (data not shown).

rAAV foci form in close contact with cellular MRN complex and MDC1

Given the ss nature of AAV genomes and the existence of regions of secondary DNA structure such as the viral ITRs within the vectors, we wanted to establish whether a relationship existed between the formation of rAAV foci and the localization of the proteins of the MRN complex, which is known to bind both ss and dsDNA and to have a pivotal role in sensing damaged or hairpin-structured DNA (D'Amours and Jackson, 2002). We observed that a vast proportion (>70%) of rAAV foci colocalized to the nuclear foci that NBS1, MRE11 and RAD50 form after HU-induced DNA damage (see Fig. 3A,C and D, respectively, for representative images and Fig. 3F for quantification). In addition, most rAAV foci

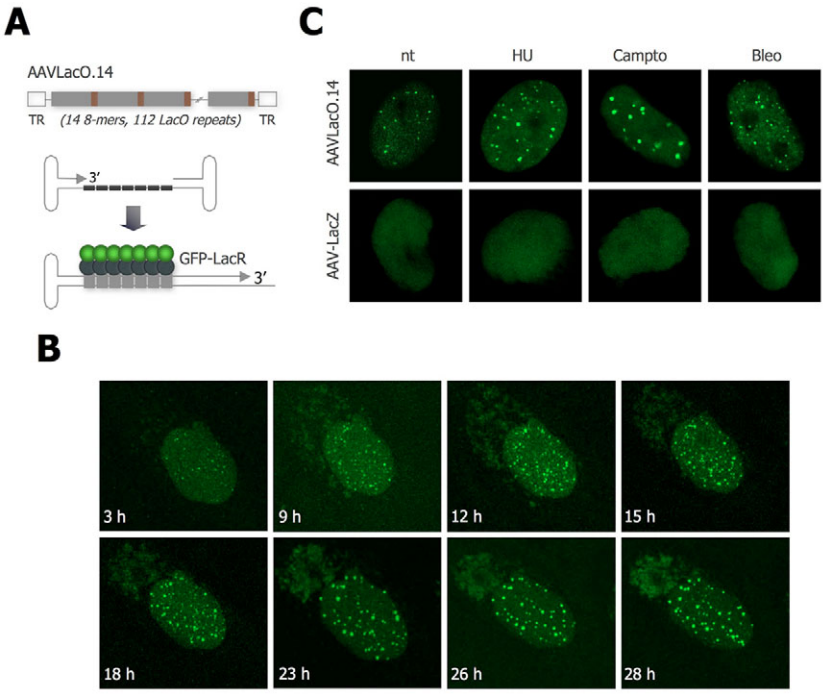

Fig. 1. Visualization of the nuclear sites of ss to ds AAVLacO.14 conversion (rAAV foci) in live GFP-LacR cells. (A) AAVLacO.14 contains the AAV ITRs flanking 14 copies of a sequence corresponding to an 8-mer of the Lac operator sequence cassette (LacO), for a total of 112 LacR binding sites. Inside the transduced cells, the GFP-LacR protein only binds the vector genome after its conversion to dsDNA. (B) Selected images from a time-lapse series of an individual MRC/GFP-LacR cell treated with HU and observed from 3 to 28 hours post infection (p.i.). The location of rAAV foci was monitored through a z-series of images. Along the z axis, images of nuclei were captured at 0.25 μm intervals, and the final images were obtained by projection of the individual sections. A movie showing the formation of these foci in real time is presented in the supplementary material Movie 1. (C) Formation of rAAV foci in MRC/GFP-LacR cells transduced with AAVLacO.14 but not with AAV-LacZ. Representative images taken 24 hours after transduction with the same amounts of vector are shown. Cells were either untreated (nt) or treated with hydroxyurea (HU), camptothecin (campto) or bleomycin (bleo), in conditions known to increase the efficiency of rAAV transduction (Zentilin et al., 2001) (see also Materials and Methods).

colocalized with NBS1 or MRE11 foci in the few cells that showed a speckled NBS1 or MRE11 localization in the absence of DNA damage (Fig. 3A,C). Furthermore, in both treated and untreated cells, rAAV foci specifically colocalized with NBS1 phosphorylated at serine 343 (P-S343-NBS1; Fig. 3B), a marker of protein activation after DNA damage (Gatei et al., 2000; Lim et al., 2000; Wu et al., 2000). Similar findings were obtained in both HeLa/GFP-LacR and MRC5/GFP-LacR cells and upon cell treatment with HU or camptothecin (Fig. 3D,E and data not shown).

AAVLacO.14 foci were also found in close proximity to the foci at which the MDC1 protein accumulates, in both untreated cells and in cells treated with camptothecin to induce DNA damage (Fig. 3E). MDC1 is known to control cellular responses to DNA damage, in part by interacting with the MRN complex and, more specifically, by mediating the transient interaction of NBS1 with DSBs and its phosphorylation by ATM (Goldberg et al., 2003; Lukas et al., 2004; Stewart et al., 2003; Xu and Stern, 2003).

MRE11 associates with rAAV genomes

To directly assess the possibility that MRN proteins might physically interact with rAAV genomes, we performed chromatin immunoprecipitation (ChIP) experiments using specific antibodies to MRE11, NBS1, P-S343-NBS1 and the cellular transcription factor USF. Cross-linked and sonicated chromatin from uninfected cells (not shown) or cells transduced with AAV-LacZ at 8, 16 and 24 hours after transduction, either in the presence or absence of HU treatment, was immunoprecipitated with each antibody; the amount of cross-linked DNA specific for rAAV or for two cellular genomic loci was then assessed by real-time PCR. One of the analyzed genomic regions (B48) contains a binding site for USF and served

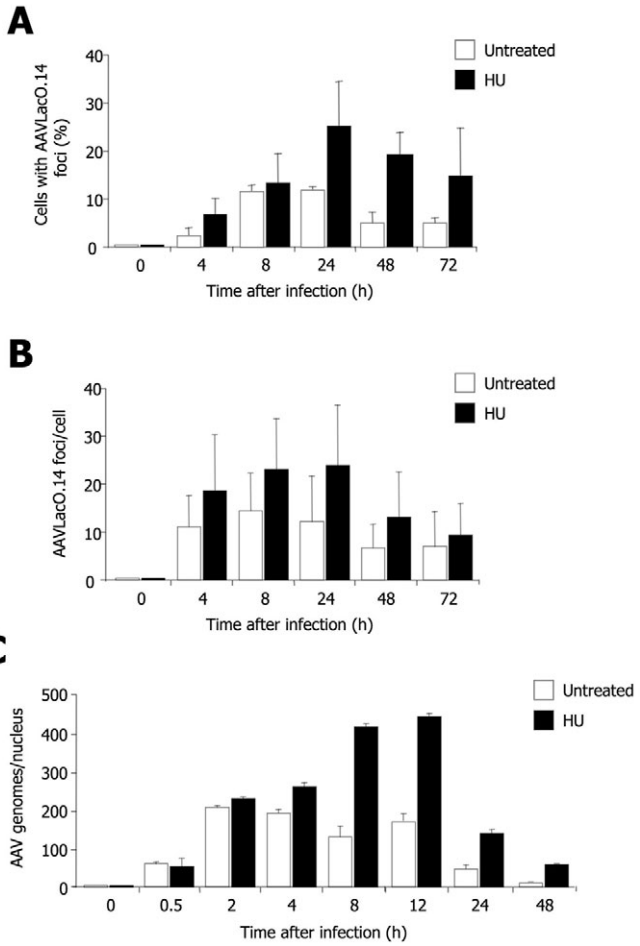

Fig. 2. Kinetics of rAAV foci formation and nuclear accumulation of rAAV genomes. (A,B) MRC5/GFP-LacR were transduced with AAVLacO.14 either without or after treatment with HU. Live cells were analyzed at different times p.i. by counting the number of cells displaying rAAV foci (A) and the number of foci per cell (B). The mean ± s.d. of 30-60 cells per time point are shown. (C) Cells were transduced with AAV-LacZ either without or after treatment with HU. Nuclear fractions were isolated at different times p.i. and the amount of rAAV genomes in nuclear fractions was determined by real-time quantitative PCR. The mean ± s.d. per time point is shown. Purity of nuclear fractions was confirmed by western blot analysis (see supplementary material Fig. S1).

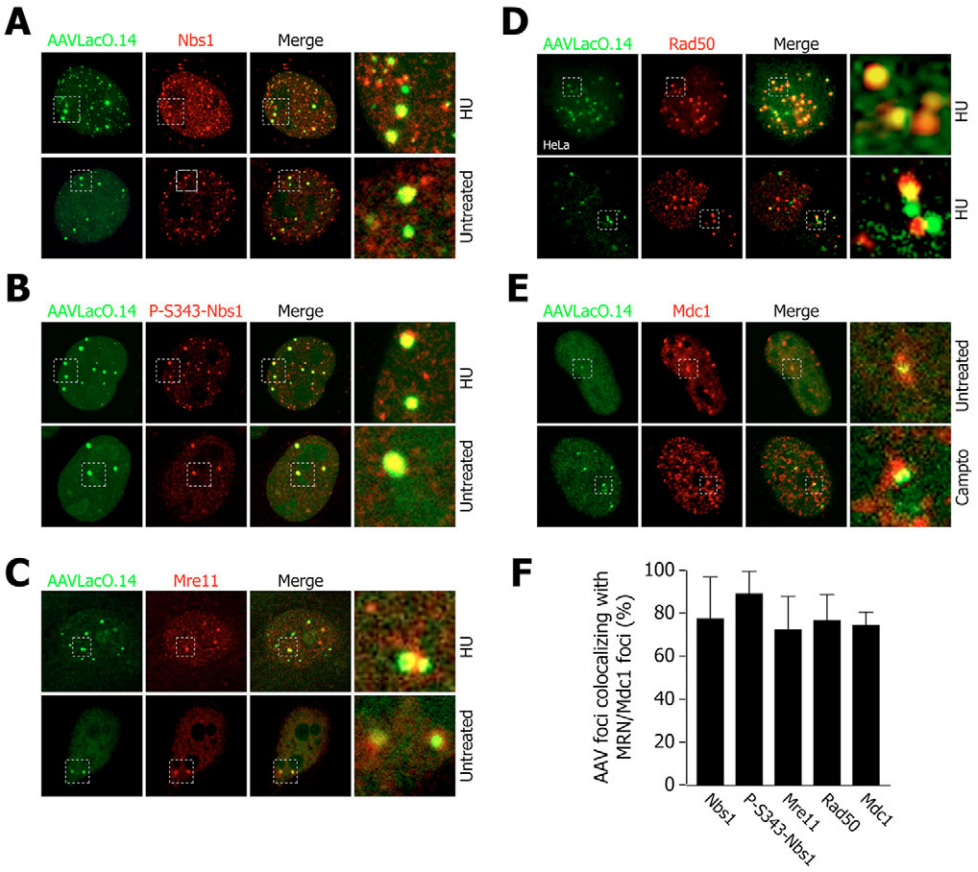

Fig. 3. Colocalization of rAAV foci with DNA-damage-response proteins. (A-E) MRC/GFP-LacR or HeLa/GFP-LacR (where indicated) cells were transduced with AAVLacO.14 and, after 24 hours, fixed and immunostained with anti-NBS1 (Nbs1; A), P-S343-NBS1 (B), MRE11 (Mre11; C), RAD50 (Rad50; D) and MDC1 (Mdc1; E) antibodies. HU and campto: cells that were treated with hydroxyurea (1 mM overnight) or camptothecin (1 nM for 6 hours) prior to AAVLacO.14 transduction. The dotted rectangles indicate the portions of the merged figures enlarged in the rightmost panels. Representative cells of at least 50 analyzed per condition are shown. (F) Number of rAAV foci colocalizing with MRN and MDC1 foci. Quantifications were performed for cells treated with HU (NBS1, P-S343-NBS1, MRE11 and RAD50) or camptothecin (MDC1) as in A-E.

as a positive control (Lusic et al., 2003). The anti-USF antibody was indeed found to specifically enrich for this region (~25 times over background), irrespective of HU treatment, in agreement with previously published findings (Todorovic et al., 2005); no enrichment was detected for rAAV DNA (Fig. 4A). The antibody against MRE11, which represents the DNA binding component of MRN, was found to specifically enrich for rAAV DNA at 8 hours (approximately sixfold) and, most remarkably, at 16 hours and 24 hours after transduction (over 45-fold at both time points) in the absence of HU treatment (Fig. 4B). However, the extent of enrichment (~2.5-, 14- and 15-fold at 8, 16 and 24 hours, respectively) was significantly lower after cell treatment with HU. The observation that MRE11 associates with rAAV genomes in the absence of HU and that the extent of binding decreases upon HU treatment is consistent with the possibility that MRN might be involved in rAAV DNA processing and then become displaced from rAAV DNA upon induction of global cellular DNA damage. In similar ChIP experiments, antibodies against both NBS1 and P-S343-NBS1 scored negative, suggesting either that NBS1 is not in such close proximity to DNA to allow effective cross-linking or it is not available to antibodies once embedded in the chromatin crosslinks.

MRN proteins inhibit formation of rAAV foci

To test the functional significance of MRN and MDC1 protein interaction with rAAV genomes, we knocked down NBS1 and MDC1 expression by RNA interference prior to cell transduction with AAVLacO.14, or with control AAV-LacZ and AAV-GFP vectors. After NBS1 silencing to less than 10% of control (Fig. 5A), the number of cells with rAAV foci was markedly increased as compared with control cells treated with an unrelated siRNA against luciferase. This effect was very evident at both 16 hours and 24 hours after transduction and in the presence or absence of HU treatment (Fig. 5C). At 24 hours after transduction and in the absence of HU, there were 41.08±9.93% of cells with rAAV foci after treatment with the anti-NBS1 siRNA, compared with 10.35±4.75% of cells with foci upon treatment with the control siRNA (representative images are shown in Fig. 5B). Of interest, the effect of HU on the number of cells with rAAV foci was less pronounced at 24 hours after transduction as compared with 16 hours (1.26-fold increase in the number of foci upon HU treatment at 24 hours, 3.19-fold increase at 16 hours), showing that the mechanism by which HU induces rAAV foci formation is saturable when NBS1 is knocked down.

In contrast to the number of cells showing rAAV foci, the total number of foci per cell, which had quite an ample range similar to that observed in MRC5 cells (Fig. 2B), was less sensitive to either HU treatment or NBS1 knock down, and differences were not significant (Fig. 5D). These results reinforce the notion that both NBS1 silencing and HU treatment act by increasing the efficiency and kinetics of rAAV foci formation but do not significantly alter the frequency at which these structures are formed.

NBS1 and MDC1 proteins inhibit rAAV transduction

Next we wanted to evaluate whether the increase in the number of cells with detectable rAAV foci upon NBS1 knock down correlated with improved rAAV vector efficiency. MRC5 and HeLa cells in which the NBS1 gene had been knocked down were significantly more permissive to transduction with the AAV-LacZ vector at different m.o.i.s, both in the presence and absence of HU (Fig. 6A,B). This finding further supports the conclusion that permissivity to rAAV transduction correlates with the number of cells with rAAV foci, and thus with the levels of dsDNA genomes inside the nucleus of the cell.

We further confirmed that NBS1 limits rAAV transduction by transducing NBS1-ILB1 cells, which are primary human

fibroblasts mutated in both copies of the NBS1 gene, as well as the same cells complemented with full length Nbs1 (Cerosaletti et al., 2000). In agreement with the siRNA results, NBS1-ILB1 fibroblasts complemented with NBS1 were less permissive to rAAV transduction when compared with the non-complemented parental cells (Fig. 6C). In contrast to wild-type MRC5, NBS1 silencing was found to have no effect in AT5 ($ATM^{-/-}$) cells, which are known to be highly permissive to rAAV transduction and to respond marginally to HU treatment (Zentilin et al., 2001) (Fig. 6D). This result is in keeping with the possibility that the negative role of NBS1 on AAV transduction might require functional ATM.

Very similar results were also observed after knocking down the expression of MDC1. For these experiments, we took advantage of the availability of stable HeLa cell clones transduced with retroviral vectors expressing short hairpin RNAs against either MDC1 or against control β-galactosidase (Lukas et al., 2004). The cell clone in which MDC1 was knocked down was significantly more permissive to AAV-GFP transduction, both in the absence or following HU treatment (Fig. 6E). Similar results were also obtained when HeLa cells where transiently transfected with synthetic siRNAs against MDC1 (Fig. 6F).

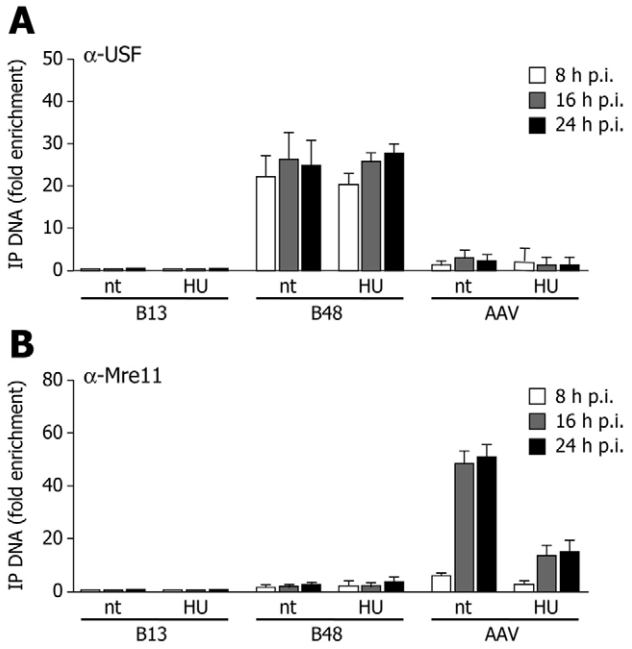

Fig. 4. Chromatin immunoprecipitation (ChIP) detects MRE11 (Mre11) bound to rAAV genomes. (A) Cross-linked chromatin at 8, 16 and 24 hours after infection with AAV-LacZ was sonicated and immunoprecipitated with an anti-USF antibody. Co-immunoprecipitated DNA was quantified by real-time PCR using primer pairs and probes in the cellular lamin B2 locus, B48 and B13, and rAAV DNA. B48 is located within the lamin B2 origin of DNA replication, which also encompasses the promoter region of the mitochondrial inner membrane translocase 13 (TIMM13) gene that contains a USF binding site; B13 is 5 kb away from the lamin B2 origin, in a region not containing any gene (Todorovic et al., 2005). The results of these quantifications are expressed as fold enrichment over B13, after normalization for the total amount of input chromatin, as already described (Lusic et al., 2003). The results show that transcription factor USF bound the B48 region, but not B13 or rAAV DNA, irrespective of HU treatment, at 8, 16 and 24 hours p.i. (B) Same as in A but using an antibody against MRE11. The protein was found to specifically bind rAAV DNA, especially at 16 and 24 hours after infection; this interaction was significantly decreased in cells pre-treated with HU.

Discussion

In this study we have exploited live imaging microscopy to assess the kinetics of ss to ds rAAV DNA generation in the nucleus of cells transduced with rAAV vectors, in the absence of viral replication or expression of any helper gene product. We observed that rAAV dsDNA accumulation does not occur diffusely in the nucleoplasm, but is confined to specific rAAV foci, which become detectable as early as 3 hours after cell infection and progressively increase in size and intensity of fluorescence over the first 12 hours after infection, suggestive of a progressive accumulation of viral dsDNA genomes into these structures. Based on the quantification of the number of rAAV genomes per nucleus and the analysis of the fluorescence intensity of the foci, we estimate that each rAAV nuclear focus contains an average of rAAV genomes that is no greater than ~20. These genomes most likely correspond to the multimerized rAAV DNA forms detected by other studies that analyzed the molecular nature of transcription-competent AAV genomes in the transduced cells (Afione et al., 1996; Yang et al., 1999).

Treatment of cells with HU is known to significantly boost the efficiency of rAAV transduction (Russell et al., 1995; Zentilin et al., 2001). In our experiments, we observed that the same

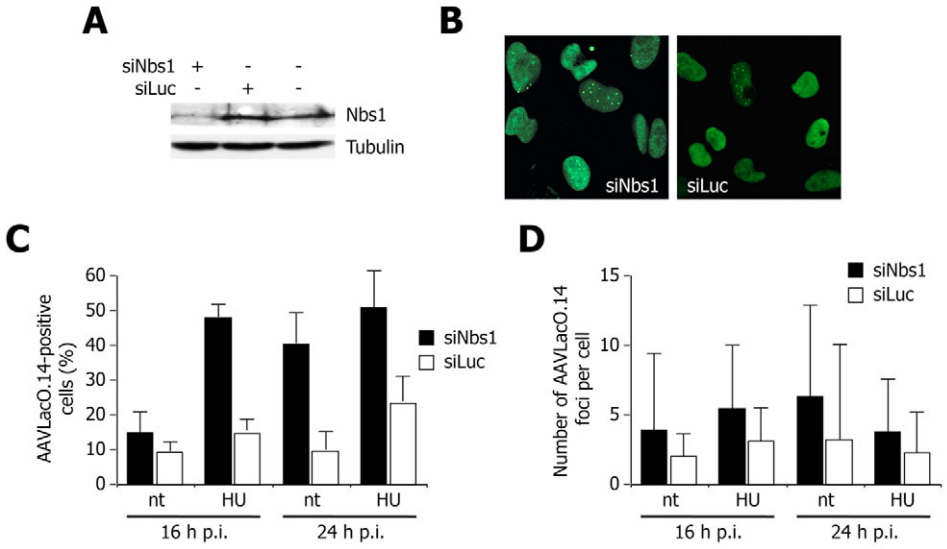

Fig. 5. Silencing of NBS1 increases formation of rAAV foci. (A) Western blotting showing the levels of NBS1 in HeLa cells after treatment with siRNAs against NBS1 (siNbs1) or luciferase (siLuc) at 60 hours after siRNA transfection (corresponding to 24 hours p.i.). The western blotting against tubulin was used as a loading control. (B) Representative images of cells treated with anti-NBS1 or anti-Luc siRNAs followed by transduction with AAV-LacO.14. The images were taken at 24 hours p.i. without HU treatment. (C) Percentage of HeLa cells with detectable AAVLacO.14 foci after silencing of NBS1. Cells were evaluated for the presence of rAAV foci 16 and 24 hours after transduction, in the presence or absence of HU treatment, as indicated. (D) Number of AAVLacO.14 foci per cell after silencing of NBS1. Conditions were the same as in C.

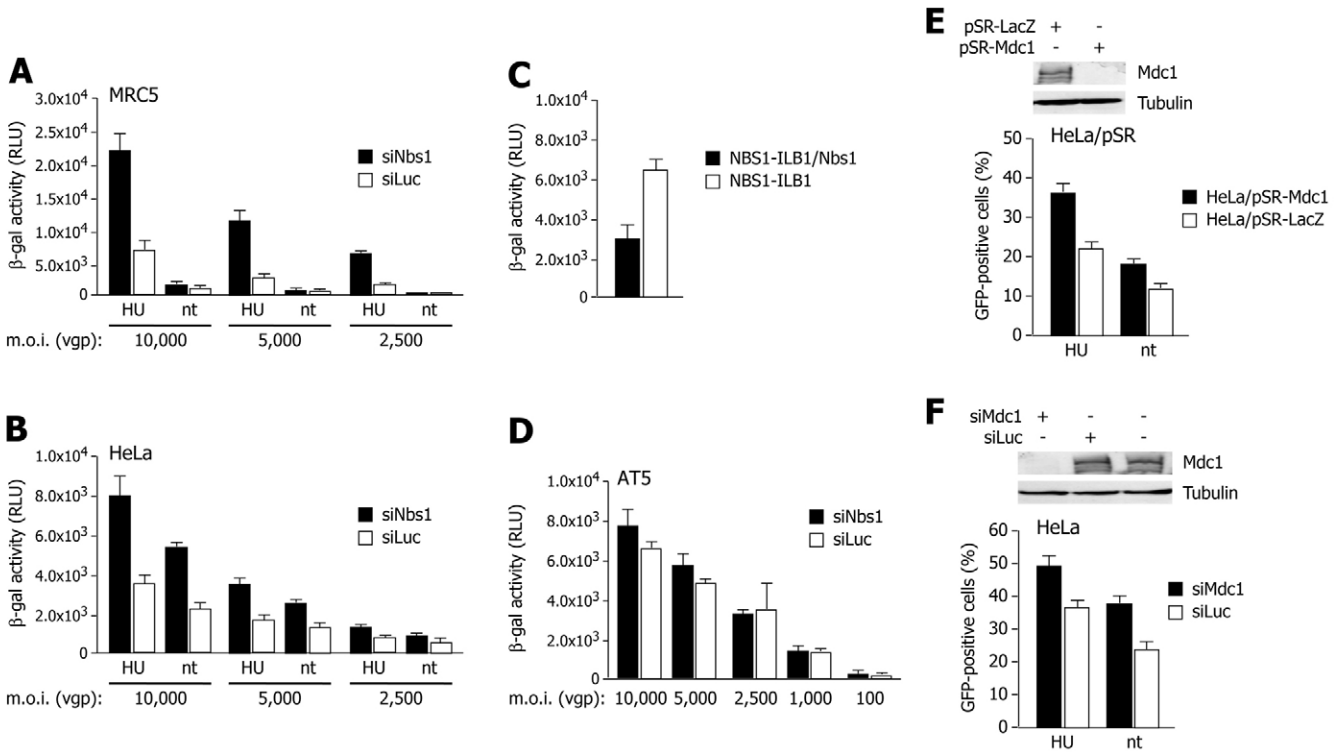

Fig. 6. Silencing of NBS1 or MDC1 increases rAAV transduction. (A) β-galactosidase activity measured as relative light units (RLU) in lysates from MRC5 cells after treatment with siRNAs against NBS1 (siNbs1) or luciferase (siLuc), followed by transduction with AAV-LacZ at three multiplicities of infection [m.o.i.; 10000, 5000 and 2500 viral genome particles (vgp) per cell]. Cells were either not treated or were treated overnight with 5 mM HU. (B) Same as in A but using HeLa cells. (C) Efficiency of AAV-LacZ (10,000 vgp/cell) transduction (measured as above) of NBS1-ILB1 cells (mutated in both copies of the NBS1 gene) and NBS1-ILB1/NBS1 cells (in which NBS1 function had been complemented by transfection of full length NBS1). (D) Same as in panel A but using AT5 cells, without HU treatment. (E) Flow cytometry analysis of retrovirally transduced HeLa cells expressing shRNAs against MDC1 (pSR-Mdc1) or β-gal (pSR-LacZ) after infection with AAV-GFP. The upper panel shows the levels of MDC1 protein in the two cell lines. (F) Flow cytometry analysis of HeLa cells transfected with siRNAs against MDC1 (siMdc1) or luciferase. The upper panel shows the levels of MDC1 protein 60 hours after siRNA transfection (24 hours after AAV-GFP transduction).

treatment also increased the number of cells with rAAV foci, thus showing that the formation of rAAV foci positively correlates with the efficiency of effective transduction. Analysis of the accumulation of rAAV genomes inside the nucleus in the presence and absence of HU treatment and at several time points suggests that the majority of the viral genomes are already inside the cell nucleus at 4 hours after infection. Although the number of viral genomes (ss and ds) reaches its maximum level at 12 hours p.i., the highest number of cells with foci is observed at 24 hours p.i., and then gradually decreases. This discrepancy is likely due to the fact that, at early time points, most of the viral genomes are present as ssDNA and possibly still protected by the viral capsids (Bartlett et al., 2000; Lux et al., 2005); at later time points, a proportion of these genomes are converted to dsDNA while the others are most likely targeted by cellular factors and eventually degraded.

Previous studies in adenovirus-infected cells, using immunofluorescence and in situ hybridization, have shown that, during infection, wt AAV DNA and proteins accumulate in discrete nuclear foci (Weitzman et al., 1996; Wistuba et al., 1997). Similar findings have been confirmed in live cells infected with HSV-1, using a rAAV vector containing 40 LacO repeats and a reporter protein similar to ours (Fraefel et al., 2004). The presence of these foci has been interpreted as an indication of the existence of subnuclear compartments in which AAV DNA replication takes place, by virtue of the colocalization, within the same replication centers, of the AAV Rep proteins, of the replicative proteins of the helper virus and of the helper virus DNA (Fraefel et al., 2004; Weitzman et al., 1996). The rAAV foci we detected in our experiments might well be coincident with these AAV and adenovirus replication centers. In this respect, however, it should be emphasized that the rAAV foci that we observed are not determined by the subnuclear localization of the replicative proteins of either AAV or helper virus, thus indicating that rAAV DNA is itself recognized by nuclear factors of cellular origin.

Indeed, we found that the rAAV foci colocalize with the nuclear compartments where the components of the MRN complex accumulate upon DNA damage. In support of the notion that these proteins are actively involved in a DNA repair process, we observed that the NBS1 foci were also detected by an antibody specific for a DNA-damage-activated form of NBS1, phosphorylated at serine 343, (Gatei et al., 2000; Lim et al., 2000; Wu et al., 2000). In keeping with the possibility that the DNA-double-strand-break repair pathway is involved in rAAV genome processing, we found that an upstream mediator, MDC1, known to increase the retention of NBS1 at the sites of DNA damage (Lukas et al., 2004), also formed foci that colocalized with rAAV foci.

What might be the role of the MRN proteins and of MDC1 in rAAV genome processing? Our RNAi experiments clearly suggest

that the overall effect of these proteins is inhibitory in rAAV dsDNA formation. Silencing of NBS1 by RNAi increased the number of cells containing rAAV foci and significantly improved the permissivity of both HeLa and MRC5 cells to transduction, again indicating that generation of dsDNA, and thus formation of rAAV foci, positively correlates with the efficiency of transduction. Similar considerations also apply to the silencing of MDC1. Interestingly, the NBS1 knock down had a marked effect in increasing the number of cells with rAAV foci; however, in each of the positive cells we observed no significant changes in the average number of foci present per cell. This observation is consistent with an effect of MRN and related proteins on the overall rate of ss to dsDNA conversion (a reduction in the intensity of fluorescence of the individual rAAV foci determines the microscopic detection of a lower number of cells presenting rAAV foci over the diffuse EGFP-LacR background), rather than with a specific effect on the mechanism of rAAV foci formation. The conclusion that proteins of the MRN complex are inhibitory for rAAV transduction is further supported by our observation that NBS1-mutated fibroblasts are more permissive to rAAV transduction when compared with the same fibroblasts complemented with full length NBS1 cDNA, as well as by the findings of M. Weitzman and collaborators, who observed that degradation of MRN by the adenovirus E1b55K/E4Orf6 markedly increases both rAAV transduction and rAAV foci formation (Schwartz et al., 2007). In keeping with these observations, chromatin immunoprecipitation experiments clearly demonstrated that MRE11, the DNA binding component of MRN, directly interacts with the rAAV genomes and that this interaction is diminished when cells are treated with DNA-damaging agents. These findings are fully in agreement with the increase in transduction and foci formation observed after induction of DNA damage.

Over the last few years, we and others have reported that cells lacking functional ATM are markedly more permissive to rAAV transduction (Sanlioglu et al., 2000; Zentilin et al., 2001). The observation that the knock down of NBS1 has no apparent effect in ATM-defective cells is consistent with the possibility that the ATM protein might mediate the negative regulation of MRN on the incoming rAAV genomes. In this respect, it has been observed that, after ionizing radiation, NBS1 is phosphorylated by ATM at serine 343 and that the S-phase checkpoint is abrogated in mutants lacking this ATM phosphorylation site (Lim et al., 2000). It is worth noting that ATM and NBS1 have been recently shown to be essential in the formation of the replication protein A-coated ssDNA microcompartments that follow cell irradiation with ionizing radiations (Bekker-Jensen et al., 2006). It might thus be envisioned that these proteins also participate in the processing of the ssDNA AAV genomes.

Together these results support the following model. On entering the nucleus, rAAV genomes, by virtue of both their ssDNA nature and the presence of the viral ITRs, are recognized by cellular DDR proteins, including MRN and MDC1. These proteins are inhibitory of ss to ds genome conversion, impeding rAAV dsDNA production or routing the genomes to aberrant processing or nucleolytic degradation, thus limiting transduction. Once this inhibition is overcome, the genomes are converted to dsDNA either by second strand DNA synthesis or direct annealing of the incoming vector complementary DNA strands (Fisher et al., 1996; Hauck et al., 2004). Cell treatment with DNA damaging agents and infection with adenovirus both have a positive effect on transduction; the former treatment diverts the inhibitory proteins away from the rAAV genomes, the latter triggers their degradation.

After ss to dsDNA conversion, the vector genome is known to undergo additional changes, mediated by host cell factors acting on the AAV ITR ends (McCarty et al., 2004). Recent work exploiting self-complementary rAAV vectors (which bypass the ss to dsDNA conversion step) has shown that ATM and MRN proteins participate in genome circularization (Choi et al., 2006). Thus, it might be envisioned that these proteins become positive factors when dsDNA conversion has already occurred. At this stage, resolution of the secondary structures in the ITRs by promoting circularization or multimerization might be essential to allow stable maintenance of the viral genomes inside the nucleus.

Materials and Methods

Cell cultures

HeLa, MRC5 and AT5, HeLa pSuper-Retro-MDC1 and HeLa pSuper-Retro-LacZ cell lines were cultured in Dulbecco's modified Eagle's medium (DMEM) supplemented with 10% fetal bovine serum. Transformed NBS-ILB1 and NBS1-ILB1/NBS1 fibroblasts (kindly provided by M. Zdzienicka, Leiden University, The Netherlands) were cultured in DMEM with 5% FBS. HeLa LacR-GFP and MRC5 LacR-GFP stably transfected cell lines were cultured as mentioned above in the presence of 300 μg/ml and 100 μg/ml hygromycin, respectively.

Plasmids and transfection

The plasmid p3′ssdEGFP, which expresses GFP linked to the *lac* repressor (LacR) and containing a nuclear localization signal, and pSV2dhfr 8.32, which contains 10 kb of 292 bp *lac* operator repeat (LacO), were kindly provided by A. S. Belmont (University of Illinois, IL). The plasmid pCMV-MCS (Stratagene, La Jolla, CA, USA) was digested with *Not*I to excise the multiple cloning site and substitute it with a multiple cloning site containing *Not*I, *Sal*I, *Eco*RI, *Xho*I, *Bam*HI and *Not*I to obtain plasmid pMCS3′. The 292 bp LacO repeat, obtained by digesting pSV2dhfr 8.32 with *Eco*RI, was cloned into the *Eco*RI site of pMCS3′; the 8-mer repeat was then amplified by directional cloning (Robinett et al., 1996) to obtain a vector containing 14 LacO repeats, for a total of 112 LacR binding sites. The 14 LacO repeats were cloned into the *Not*I site of pAAV-MCS to generate pAAVLacO.14. To obtain stable clones expressing the LacR fused to GFP, HeLa and MRC5 cells were transfected with Polyfect transfection reagent (Qiagen GmbH, Hilden, Germany) and clones were selected with hygromycin (300 μg/ml for HeLa cells; 100 μg/ml for MRC5).

Production of rAAV stocks

The rAAV vectors used in this study were produced from pTR-UF5 (AAV-GFP), kindly provided by N. Muzyczka (University of Florida College of Medicine, FL), pAAV-LacZ (Stratagene) and pAAVLacO.14. Cloning and propagation of AAV plasmids was carried in XL-10 Gold *E. coli* strain (Stratagene, La Jolla, CA, USA). Infectious AAV vector particles were generated by the AAV Vector Unit (AVU) at ICGEB Trieste (http://www.icgeb.org/RESEARCH/TS/COREFACILITIES/AVU.htm) in HEK293 cells, using dual plasmid cotransfection procedure with pDG as packaging helper plasmid (kindly provided by J. A. Kleinschmidt, DKFZ, Germany), as previously described (Zentilin et al., 2001). Titration of AAV-GFP and AAV-LacZ viral particles was performed by real-time PCR quantification of the number of viral genomes, as described previously (Zentilin et al., 2001); the viral preparations used in this work had titers between 1×10^{11} and 1×10^{12} viral genome particles (vgp) per ml. The titers of AAVLacO.14 were measured by Southern blotting using serial dilutions of the input pMCS3′lacO.14 plasmid as a standard; the preparations of this vector had titers between 1×10^{8} and 1×10^{9} vgp/ml.

Vector transduction experiments

Transduction with AAV-GFP was performed by plating 4×10^{5} cells in 24-well plates. In the experiments with AAVLacO.14, 2×10^{4} cells were seeded 24 hours before vector addition in eight-well chamber slides (Labtech International, Woodside, UK) or 5×10^{5} cells in 6 cm glass bottom dishes). Transduction with AAV-LacZ was performed in 96-well plates with 3×10^{3} cells per well. When indicated, cells were treated for 12-16 hours with 1 mM HU, for 6 hours with 1 nM camptothecin (Sigma-Aldrich, St Louis, MO, USA) or for 6 hours with 0.15 IU/ml bleomycin (Calbiochem) from 15 IU/ml stocks dissolved in water, before the addition of vector. Transduction with the different vectors was performed in DMEM supplemented with 10% FCS. After 3 hours incubation, cells were washed in PBS and fresh culture medium was added. Cellular GFP fluorescence was analyzed by flow cytometry using a FACSCalibur (Becton Dickinson, San Jose, CA, USA) 36 hours after AAV-GFP addition. In the case of AAV-LacZ transduction, β-galactosidase activity was determined 36 hours post-infection by measuring *o*-nitrophenyl-D-galacto-pyranoside (ONPG) cleavage using a photometric assay, as described elsewhere (Brown et al., 2000). Relative light units (RLU) were expressed as the ratio between

ONPG absorbance at 405 nm and the protein concentration (in ng/ml) of the sample, multiplied by an arbitrary factor of 1000.

Confocal microscopy

Live or fixed cultures were analyzed by confocal microscopy using a Leica TCS-SL or a Zeiss LSM 510 laser scanning microscope. The different channels were detected sequentially, and the laser power and detection windows were adjusted for each channel to exclude overlap between different fluorochromes and to avoid signal saturation. rAAV foci location was monitored through a z-series of images. For live cell recording, cells plated on 6 cm glass bottom dishes were placed in a humidified Plexiglas chamber and maintained at 37°C and 5% CO_2 throughout the experiment. The fluorescence intensity of DNA foci was measured by calculating the mean fluorescence intensities of pixels of maximum intensity projection of x,y,z,t scan and subtracting the background intensity calculated as mean fluorescence intensity outside the cell, at each time point.

Foci tracking analysis

Tracking of rAAV foci was performed as already described (Ferrari et al., 2003). Briefly, nuclei were scanned with x,y,z,t scan mode (3D + time lapse) with a Leica TCS-SL laser scanning microscope. Movement information was obtained from 2D images obtained, at each time point, from maximum intensity projections of 0.24 μm (supplementary material Fig. S1A) or 0.45 μm (supplementary material Fig. S1B-D) -thick optical z sections spanning the full depth of the nucleus. Starting from each frame, the images of the nucleus were cropped and aligned. The relative movement of each rAAV focus inside the nucleus was measured according to its x and y coordinates at each frame using the MetaMorph software and plotted with Origin Pro v7.03 (OriginLab Corp., Northampton, MA, USA). The mean velocity was calculated from the observed trajectories.

Immunofluorescence

At the indicated time points after infection, cells were washed twice with PBS and fixed and permeabilized either with 2% paraformaldehyde in PBS for 15 minutes at room temperature followed by two washes with 0.1% Triton X-100 in PBS or with 100% methanol at –20°C for 20 minutes followed by 100% acetone at –20°C for 20 seconds. After fixing, the cells were washed twice, and incubated with primary antibody for 1.5 hours in PBS plus 0.15% glycine and 0.5% BSA (PBS^+) in a moist chamber at room temperature. The following antibodies were used: mouse anti-human RAD50 (GeneTex, San Antonio, TX, USA, Ab89) diluted 1:200; mouse anti-human MRE11 (GeneTex, Ab214, 12D7) and rabbit anti-human NBS1 (Novus Biologicals, Littleton, CO, USA, Ab398, NB 100-143), rabbit anti-phospho-NBS1 (Ser343; Novus Biologicals, 100-284A3) diluted 1:500 and anti-MDC1 rabbit polyclonal serum (kindly provided by S. P. Jackson, The Wellcome Trust/Cancer Research UK Gurdon Institute, University of Cambridge, UK) diluted 1:200. Cells were incubated with the secondary antibodies for 1 hour in PBS^+ in a moist chamber at room temperature. The secondary antibodies used were goat anti-rabbit Alexa Fluor 594-conjugated and goat anti-mouse Alexa Fluor 594-conjugated (Molecular Probes, Eugene, OR, USA) both diluted 1:1000. Cells were mounted on chamber slides in Vectashield Mounting Medium (Vector Laboratories, Burlingame, CA, USA) containing 4′-6′-diamino-2-phenylidole (DAPI). Fixed cells were analyzed with a Leica DMLB fluorescence microscope connected to Leica DC camera or by confocal microscopy.

Cell fractionation and quantification of nuclear rAAV genomes

Transduction with AAV-LacZ (m.o.i. 10,000 vgp) was performed in 6 cm dishes containing 8×10^5 HeLa cells. When indicated, cells were treated for 12-16 hours with 1 mM HU before the addition of the vector. At the indicated times after infection, cytoplasmic and nuclear fractions were isolated, as described by Mendez and Stillman (Mendez and Stillman, 2000). Briefly, cells were washed once with PBS, treated with trypsin and further washed with PBS. Cell pellets were resuspended in 150 μl buffer A (10 mM Hepes pH 7.9, 10 mM KCl, 1.5 mM $MgCl_2$, 0.34 M sucrose, 10% glycerol, 1 mM DTT, protease inhibitors) after which 150 μl of buffer A containing 0.2% Triton X-100 was added. Samples were incubated for 5 minutes on ice and then centrifuged for 5 minutes at 1300 ***g*** at 4°C. Nuclear fractions (pellets) were further washed with buffer A containing 0.1% Triton X-100 and resuspended in 200 μl PBS. Total DNA was purified from nuclear fractions using DNeasy Blood and Tissue kit (Qiagen), according to the manufacturer's instructions. The amount of rAAV genome present in nuclear fractions was quantified by real-time PCR using serial dilutions of pAAV-LacZ (Stratagene) as standards, essentially as performed for the quantification of rAAV stocks. Values from the real-time PCR quantification of B13 DNA segment of the lamin B2 genomic region were used as an internal control to normalize the total DNA concentration (number of nuclei) of the different samples. Purity of nuclear fractions was confirmed by western blotting to determine the absence of α-tubulin and presence of the nuclear protein PARP (supplementary material Fig. S2).

RNA interference

Cells (4×10^5) were plates in 3.5 cm dishes and transfected using GeneSilencer (Gene Therapy Systems, San Diego, CA, USA) according to the manufacturer's recommendations. The sequence of the siRNAs against NBS1 (siNBS1), MDC1 (siMDC1), and luciferase (siLuc) were GGAAGAAACGUGAACUCAA (dTdT), CAACAAGAAGACGCGAAUC (dTdT) (Stewart et al., 2003), and CGUACGCGGAAUACUUCGA (dTdT) (Dharmacon, Lafayette, CO, USA), respectively. Twenty-four hours after siRNA transfection, cells well trypsinized and replated in 24-well plates, 96-well plates or eight-well-chambered slides and transduced with rAAV.

The pSR-MDC1 cell line is a HeLa cell derivative transduced with the pSUPER-retro retroviral vector (Brummelkamp et al., 2002) stably expressing an anti-MDC1 shRNA (insert sequence: GATCCCCGTC TCCCAGAAGA CAGTGATTCA AGAGATCACT GTCTTCTGGG AGACTTTTTG GAAA). The control pSR-LacZ cell line expresses an anti-β-galactosidase shRNA (insert sequence: AGCTTTTCCA AAAAGTCTCC CAGAAGACAG TGATCTCTTG AATCACTGTC TTCTGGGAGA CGGG) from the same vector. Both cell lines were kindly provided by Y. Shiloh (Sackler School of Medicine, Tel Aviv University, Israel).

Western blotting

Total cell lysates were prepared from cells treated with siRNA. Cells were lysed with sample buffer (20 mM Tris-HCl pH 8, 20 mM NaCl, 10% glycerol, 1% NP40, 10 mM EDTA, 2 mM PMSF, leupeptin 2.5 μg/ml, pepstatin 2.5 μg/ml) followed by heating to 100°C for 5 minutes. Protein concentration was determined by the Bradford method (BioRad, Richmond, CA); 10 μg of protein per lane were loaded on 12% SDS-PAGE minigels, and transferred to nitrocellulose (Amersham Biosciences, Bucks, UK). Immunoblots were blocked in 5% non-fat dry milk in TBST (50 mM Tris-HCl pH 7.4, 200 mM NaCl, 0.04% Tween 20). Primary antibodies were rabbit anti-α-tubulin (Sigma; diluted 1:10,000), anti-MDC1 (diluted 1:10,000), anti-NBS1 (Novus Biologicals), 100-143 (diluted 1:5,000), and anti-PARP (Santa Cruz Biotechnology, Santa Cruz, CA; sc-7150, diluted 1:200) antibodies. Horseradish peroxidase-labeled anti-rabbit antibody (Santa Cruz Biotechnology), 1:1000 was used as a secondary antibody. Antibody staining was detected using the ECL chemiluminescence system (Amersham Biosciences).

Chromatin immunoprecipitation (ChIP)

HeLa cells were transduced with AAV-LacZ at an m.o.i. of 10,000 vgp/cell. Where indicated, cells were pre-treated with 1 mM HU overnight before infection. ChIP was essentially performed as already described (Lusic et al., 2003; Todorovic et al., 2005). At 8, 16 and 24 hours after infection, cells were fixed by adding fixing solution (11% formaldehyde, 100 mM NaCl, 1 mM EDTA, 0.5 mM EGTA pH 8.0, 50 mM Tris-HCl pH 8.0) directly to the cell culture medium at 1% final concentration. Cross-linking was allowed to proceed for 10 minutes at 37°C and was stopped by the addition of glycine at a final concentration of 0.125 M. Fixed cells were washed once in ice-cold PBS, once in buffer B1 (0.25% Triton X-100, 10 mM EDTA, 0.5 mM EGTA, 10 mM Tris-HCl pH 8.0) and once in buffer B2 (1 mM EDTA, 0.5 mM EGTA, 200 mM NaCl, 10 mM Tris-HCl pH 8.0). Cells were pelletted by centrifugation and resuspended in RIPA 50 buffer [50 mM NaCl, 20 mM Tris-HCl pH 7.4, 1 mM EDTA, 0.5% Nonidet P-40 (NP-40), 0.5% deoxycholic acid, 0.1% sodium dodecyl sulfate (SDS), protease inhibitors]. Chromatin was sheared by sonication (20 pulses, 30 seconds each) on ice and centrifuged to pellet debris. Immunoprecipitations were carried out by adding 5 μl anti-USF or anti-MRE11 antibodies (Santa Cruz Biotechnology) at 4°C overnight. Immune complexes were collected with protein A-Sepharose CL-4B (Pharmacia), and beads were washed three times with 1 ml RIPA 150 buffer (same as RIPA 50 but with 150 mM NaCl). Protein-DNA complexes were resuspended in 300 μl of TE buffer and digested with 5 IU of DNase-free RNase (Roche) for 30 minutes at 37°C. Samples were then treated for 3 hours at 56°C with 300 g/ml proteinase K (Sigma) in 0.5% SDS, 100 mM NaCl, and were incubated overnight at 65°C to revert crosslinks. DNA was extracted with phenol-chloroform-isoamyl alcohol, ethanol precipitation and resuspended in water for real-time PCR quantification of two regions in the cellular lamin B2 region (B13 and B48), using already described primer pairs and TaqMan probes (Lusic et al., 2003; Todorovic et al., 2005) and for rAAV DNA (using the same primer pair and probe used for AAV titration).

The authors are grateful to Y. Shiloh, A. S. Belmont, M. Z. Zdzienicka, N. Muzyczka, J. A. Kleinschmidt for reagents, to S. P. Jackson for reagents and helpful comments and suggestions, and to A. Marcello and P. Maiuri for helpful collaboration in the fluorescence quantification experiments. M. Mano is recipient of a fellowship from the Portuguese Foundation for Science and Technology. This work was supported in part by grants from the FIRB program of MUR, Italy, from the Fondazione CRTrieste, Italy and from the Telethon Foundation, Italy to M.G. and in part by NIH grants AI43341 and CA97093 to M.D.W.

References

Afione, S. A., Conrad, C. K., Kearns, W. G., Chunduru, S., Adams, R., Reynolds, T. C., Guggino, W. B., Cutting, G. R., Carter, B. J. and Flotte, T. R. (1996). In vivo model of adeno-associated virus vector persistence and rescue. *J. Virol.* **70**, 3235-3241.

Alexander, I. E., Russell, D. W. and Miller, A. D. (1994). DNA-damaging agents greatly increase the transduction of nondividing cells by adeno-associated virus vectors. *J. Virol.* **68**, 8282-8287.

Bartlett, J. S., Wilcher, R. and Samulski, R. J. (2000). Infectious entry pathway of adeno-associated virus and adeno-associated virus vectors. *J. Virol.* **74**, 2777-2785.

Bekker-Jensen, S., Lukas, C., Kitagawa, R., Melander, F., Kastan, M. B., Bartek, J. and Lukas, J. (2006). Spatial organization of the mammalian genome surveillance machinery in response to DNA strand breaks. *J. Cell Biol.* **173**, 195-206.

Belmont, A. S. and Straight, A. F. (1998). In vivo visualization of chromosomes using lac operator-repressor binding. *Trends Cell Biol.* **8**, 121-124.

Brown, M., Zhang, Y., Dermine, S., de Wynter, E. A., Hart, C., Kitchener, H., Stern, P. L., Skinner, M. A. and Stacey, S. N. (2000). Dendritic cells infected with recombinant fowlpox virus vectors are potent and long-acting stimulators of transgene-specific class I restricted T lymphocyte activity. *Gene Ther.* **7**, 1680-1689.

Brummelkamp, T. R., Bernards, R. and Agami, R. (2002). A system for stable expression of short interfering RNAs in mammalian cells. *Science* **296**, 550-553.

Cerosaletti, K. M., Desai-Mehta, A., Yeo, T. C., Kraakman-Van Der Zwet, M., Zdzienicka, M. Z. and Concannon, P. (2000). Retroviral expression of the NBS1 gene in cultured Nijmegen breakage syndrome cells restores normal radiation sensitivity and nuclear focus formation. *Mutagenesis* **15**, 281-286.

Choi, V. W., McCarty, D. M. and Samulski, R. J. (2006). Host cell DNA repair pathways in adeno-associated viral genome processing. *J. Virol.* **80**, 10346-10356.

D'Amours, D. and Jackson, S. P. (2002). The Mre11 complex: at the crossroads of dna repair and checkpoint signalling. *Nat. Rev. Mol. Cell Biol.* **3**, 317-327.

Dundr, M., McNally, J. G., Cohen, J. and Misteli, T. (2002). Quantitation of GFP-fusion proteins in single living cells. *J. Struct. Biol.* **140**, 92-99.

Dupre, A., Boyer-Chatenet, L. and Gautier, J. (2006). Two-step activation of ATM by DNA and the Mre11-Rad50-Nbs1 complex. *Nat. Struct. Mol. Biol.* **13**, 451-457.

Ferrari, A., Pellegrini, V., Arcangeli, C., Fittipaldi, A., Giacca, M. and Beltram, F. (2003). Caveolae-mediated internalization of extracellular HIV-1 Tat fusion proteins visualized in real time. *Mol. Ther.* **8**, 284-294.

Ferrari, F. K., Samulski, T., Shenk, T. and Samulski, R. J. (1996). Second-strand synthesis is a rate-limiting step for efficient transduction by recombinant adeno-associated virus vectors. *J. Virol.* **70**, 3227-3234.

Fisher, K. J., Gao, G. P., Weitzman, M. D., DeMatteo, R., Burda, J. F. and Wilson, J. M. (1996). Transduction with recombinant adeno-associated virus for gene therapy is limited by leading-strand synthesis. *J. Virol.* **70**, 520-532.

Fraefel, C., Bittermann, A. G., Bueler, H., Heid, I., Bachi, T. and Ackermann, M. (2004). Spatial and temporal organization of adeno-associated virus DNA replication in live cells. *J. Virol.* **78**, 389-398.

Gatei, M., Young, D., Cerosaletti, K. M., Desai-Mehta, A., Spring, K., Kozlov, S., Lavin, M. F., Gatti, R. A., Concannon, P. and Khanna, K. (2000). ATM-dependent phosphorylation of nibrin in response to radiation exposure. *Nat. Genet.* **25**, 115-119.

Glauser, D. L., Saydam, O., Balsiger, N. A., Heid, I., Linden, R. M., Ackermann, M. and Fraefel, C. (2005). Four-dimensional visualization of the simultaneous activity of alternative adeno-associated virus replication origins. *J. Virol.* **79**, 12218-12230.

Goldberg, M., Stucki, M., Falck, J., D'Amours, D., Rahman, D., Pappin, D., Bartek, J. and Jackson, S. P. (2003). MDC1 is required for the intra-S-phase DNA damage checkpoint. *Nature* **421**, 952-956.

Hauck, B., Zhao, W., High, K. and Xiao, W. (2004). Intracellular viral processing, not single-stranded DNA accumulation, is crucial for recombinant adeno-associated virus transduction. *J. Virol.* **78**, 13678-13686.

Hermonat, P. L. and Muzyczka, N. (1984). Use of adeno-associated virus as a mammalian DNA cloning vector: transduction of neomycin resistance into mammalian tissue culture cells. *Proc. Natl. Acad. Sci. USA* **81**, 6466-6470.

Lee, J. H. and Paull, T. T. (2005). ATM activation by DNA double-strand breaks through the Mre11-Rad50-Nbs1 complex. *Science* **308**, 551-554.

Lim, D. S., Kim, S. T., Xu, B., Maser, R. S., Lin, J., Petrini, J. H. and Kastan, M. B. (2000). ATM phosphorylates p95/nbs1 in an S-phase checkpoint pathway. *Nature* **404**, 613-617.

Lukas, C., Melander, F., Stucki, M., Falck, J., Bekker-Jensen, S., Goldberg, M., Lerenthal, Y., Jackson, S. P., Bartek, J. and Lukas, J. (2004). Mdc1 couples DNA double-strand break recognition by Nbs1 with its H2AX-dependent chromatin retention. *EMBO J.* **23**, 2674-2683.

Lusic, M., Marcello, A., Cereseto, A. and Giacca, M. (2003). Regulation of HIV-1 gene expression by histone acetylation and factor recruitment at the LTR promoter. *EMBO J.* **22**, 6550-6561.

Lux, K., Goerlitz, N., Schlemminger, S., Perabo, L., Goldnau, D., Endell, J., Leike, K., Kofler, D. M., Finke, S., Hallek, M. et al. (2005). Green fluorescent protein-tagged adeno-associated virus particles allow the study of cytosolic and nuclear trafficking. *J. Virol.* **79**, 11776-11787.

McCarty, D. M., Young, S. M., Jr and Samulski, R. J. (2004). Integration of adeno-associated virus (AAV) and recombinant AAV vectors. *Annu. Rev. Genet.* **38**, 819-845.

Mendez, J. and Stillman, B. (2000). Chromatin association of human origin recognition complex, cdc6, and minichromosome maintenance proteins during the cell cycle: assembly of prereplication complexes in late mitosis. *Mol. Cell. Biol.* **20**, 8602-8612.

Robinett, C. C., Straight, A., Li, G., Willhelm, C., Sudlow, G., Murray, A. and Belmont, A. S. (1996). In vivo localization of DNA sequences and visualization of large-scale chromatin organization using lac operator/repressor recognition. *J. Cell Biol.* **135**, 1685-1700.

Russell, D. W., Alexander, I. E. and Miller, A. D. (1995). DNA synthesis and topoisomerase inhibitors increase transduction by adeno-associated virus vectors. *Proc. Natl. Acad. Sci. USA* **92**, 5719-5723.

Sanlioglu, S., Benson, P. and Engelhardt, J. F. (2000). Loss of ATM function enhances recombinant adeno-associated virus transduction and integration through pathways similar to UV irradiation. *Virology* **268**, 68-78.

Schwartz, R. A., Palacios, J. A., Cassell, G. D., Adam, S., Giacca, M. and Weitzman, M. D. (2007). The Mre11/Rad50/Nbs1 complex limits adeno-associated virus transduction and replication. *J. Virol.* **81**, 12936-12945.

Seno, J. D. and Dynlacht, J. R. (2004). Intracellular redistribution and modification of proteins of the Mre11/Rad50/Nbs1 DNA repair complex following irradiation and heat-shock. *J. Cell. Physiol.* **199**, 157-170.

Shiloh, Y. (2003). ATM and related protein kinases: safeguarding genome integrity. *Nat. Rev. Cancer* **3**, 155-168.

Stewart, G. S., Wang, B., Bignell, C. R., Taylor, A. M. and Elledge, S. J. (2003). MDC1 is a mediator of the mammalian DNA damage checkpoint. *Nature* **421**, 961-966.

Straight, A. F., Marshall, W. F., Sedat, J. W. and Murray, A. W. (1997). Mitosis in living budding yeast: anaphase A but no metaphase plate. *Science* **277**, 574-578.

Todorovic, V., Giadrossi, S., Pelizon, C., Mendoza-Maldonado, R., Masai, H. and Giacca, M. (2005). Human origins of DNA replication selected from a library of nascent DNA. *Mol. Cell* **19**, 567-575.

Tratschin, J. D., Miller, I. L. and Carter, B. J. (1984). Genetic analysis of adeno-associated virus: properties of deletion mutants constructed in vitro and evidence for an adeno-associated virus replication function. *J. Virol.* **51**, 611-619.

Tsukamoto, T., Hashiguchi, N., Janicki, S. M., Tumbar, T., Belmont, A. S. and Spector, D. L. (2000). Visualization of gene activity in living cells. *Nat. Cell Biol.* **2**, 871-878.

Tumbar, T., Sudlow, G. and Belmont, A. S. (1999). Large-scale chromatin unfolding and remodeling induced by VP16 acidic activation domain. *J. Cell Biol.* **145**, 1341-1354.

van den Bosch, M., Bree, R. T. and Lowndes, N. F. (2003). The MRN complex: coordinating and mediating the response to broken chromosomes. *EMBO Rep.* **4**, 844-849.

Weitzman, M. D., Fisher, K. J. and Wilson, J. M. (1996). Recruitment of wild-type and recombinant adeno-associated virus into adenovirus replication centers. *J. Virol.* **70**, 1845-1854.

Wistuba, A., Kern, A., Weger, S., Grimm, D. and Kleinschmidt, J. A. (1997). Subcellular compartmentalization of adeno-associated virus type 2 assembly. *J. Virol.* **71**, 1341-1352.

Wu, X., Ranganathan, V., Weisman, D. S., Heine, W. F., Ciccone, D. N., O'Neill, T. B., Crick, K. E., Pierce, K. A., Lane, W. S., Rathbun, G. et al. (2000). ATM phosphorylation of Nijmegen breakage syndrome protein is required in a DNA damage response. *Nature* **405**, 477-482.

Xu, X. and Stern, D. F. (2003). NFBD1/MDC1 regulates ionizing radiation-induced focus formation by DNA checkpoint signaling and repair factors. *FASEB J.* **17**, 1842-1848.

Yang, J., Zhou, W., Zhang, Y., Zidon, T., Ritchie, T. and Engelhardt, J. F. (1999). Concatamerization of adeno-associated virus circular genomes occurs through intermolecular recombination. *J. Virol.* **73**, 9468-9477.

Zentilin, L., Marcello, A. and Giacca, M. (2001). Involvement of cellular double-stranded DNA break binding proteins in processing of the recombinant adeno-associated virus genome. *J. Virol.* **75**, 12279-12287.

Zhou, C., Yang, Q. and Trempe, J. P. (1999). Enhancement of UV-induced cytotoxicity by the adeno-associated virus replication proteins. *Biochim. Biophys. Acta* **1444**, 371-383.